# Process Development of C–N Cross-Coupling and Enantioselective Biocatalytic Reactions for the Asymmetric Synthesis of Niraparib

**ARTICLE** *in* ORGANIC PROCESS RESEARCH & DEVELOPMENT · OCTOBER 2013

Impact Factor: 2.53 · DOI: 10.1021/op400233z



**10 AUTHORS**, INCLUDING:

Birgit Kosjek
Merck
**25** PUBLICATIONS **789** CITATIONS
SEE PROFILE

Guy Humphrey
Merck
**60** PUBLICATIONS **2,200** CITATIONS
SEE PROFILE

Khateeta M. Emerson
**16** PUBLICATIONS **217** CITATIONS
SEE PROFILE

Organic Process Research & Development

Article

pubs.acs.org/OPRD

# Process Development of C−N Cross-Coupling and Enantioselective Biocatalytic Reactions for the Asymmetric Synthesis of Niraparib

Cheol K. Chung,*[,†] Paul G. Bulger,*[,†] Birgit Kosjek,[†] Kevin M. Belyk,[†] Nelo Rivera,[†] Mark E. Scott,[‡] Guy R. Humphrey,[†] John Limanto,[†] Donald C. Bachert,[§] and Khateeta M. Emerson[§]

[†]Department of Process Chemistry, Merck & Co., Inc., Rahway, New Jersey 07065, United States

[‡]Department of Medicinal Chemistry, Merck & Co., Inc., Boston, Massachusetts 02115, United States

[§]Department of Chemical Process Development and Commercialization, Merck & Co., Inc., Rahway, New Jersey 07065, United States

Supporting Information

**ABSTRACT:** Process development of the synthesis of the orally active poly(ADP-ribose)polymerase inhibitor niraparib is described. Two new asymmetric routes are reported, which converge on a high-yielding, regioselective, copper-catalyzed *N*-arylation of an indazole derivative as the late-stage fragment coupling step. Novel transaminase-mediated dynamic kinetic resolutions of racemic aldehyde surrogates provided enantioselective syntheses of the 3-aryl-piperidine coupling partner. Conversion of the C−N cross-coupling product to the final API was achieved by deprotection and salt metathesis to isolate the desired crystalline salt form.

## INTRODUCTION

The enzyme poly(ADP-ribose)polymerase (PARP) is involved in a number of cellular processes, one of these being to assist in the repair of single-strand breaks in DNA. Overexpression of the PARP enzyme in certain cancer types has been implicated in cancer cell proliferation and tumor progression.[1] Consequently, inhibitors of PARP are of significant interest in the oncology field, with a number of small-molecule agents having been entered into clinical trials.[2] A recent report[3] from these laboratories described the development of a kilogram-scale synthesis of niraparib *p*-toluenesulfonate monohydrate (**9**, Scheme 1), an orally active PARP inhibitor shown to be efficacious in murine xenograft cancer models.[4] This convenient route was fit-for-purpose in being amenable to the production of the quantities of active pharmaceutical ingredient (API) needed to advance the compound through early preclinical evaluation and into the clinic. However, it was envisaged that more efficient, practical chemistry would subsequently be needed for significantly larger API deliveries as the program would move towards late-stage development. We describe herein the results of laboratory-scale development of alternative routes to the target compound **9**. These routes feature novel bio- and chemocatalytic transformations that build upon the foundations laid by recent advances in these areas of catalysis.

The first kilogram-scale synthesis of compound **9**, isolated as the *p*-toluenesulfonate salt monohydrate crystalline form, proceeded in 11 total steps and 11% overall yield (Scheme 1).[3] The linear sequence from commercial starting materials **1** and **2** was relatively short, but a number of opportunities were identified for longer-term route development. A primary objective was to develop an asymmetric synthesis of the piperidine unit, as the modest throughput of the chromatographic resolution was recognized to be a significant bottleneck. Evaluation of alternative fragment-coupling strategies that avoided the use of azide reagents at elevated temperature was also desirable, as was elimination of the use of chlorinated solvents, heavy transition metal catalysts (e.g., Pd, Pt), specialized equipment (pressurized hydrogenation) and silica gel purification. Furthermore, detailed investigation of structure−activity relationships had revealed that the primary amide substituent ($CONH_2$) on the indazole ring of the tetracyclic core conferred a level of potency that led to low occupational exposure limits for penultimate **8** and the API **9**. Dedicated potent compound-handling facilities would be needed for steps involving the generation, use, or handling of compounds containing the primary amide motif; thus, minimization of the number of unit operations would be beneficial. Collectively, opportunities for sizable improvements in overall yield and productivity, with concomitant reductions in cycle time, cost and environmental impact, presented themselves for the synthesis of the target compound **9**. A further demand on any new route would be that it reliably deliver material meeting exacting purity specifications with no new impurities (relative to earlier preclinical batches), including the undesired enantiomer, at levels above ICH qualification thresholds.

## RESULTS AND DISCUSSION

**General Synthetic Strategy.** Rather than attempt to optimize the existing route further, we elected to investigate a new approach which featured a C−N coupling between indazole **11** and chiral 3-aryl-piperidine **12** as the convergent

**Special Issue:** Transition Metal-Mediated Carbon-Heteroatom Coupling Reactions

**Received:** August 26, 2013
**Published:** October 25, 2013

   dx.doi.org/10.1021/op400233z | *Org. Process Res. Dev.* 2014, 18, 215−227

**Scheme 1. First kilogram-scale synthesis of compound 9**

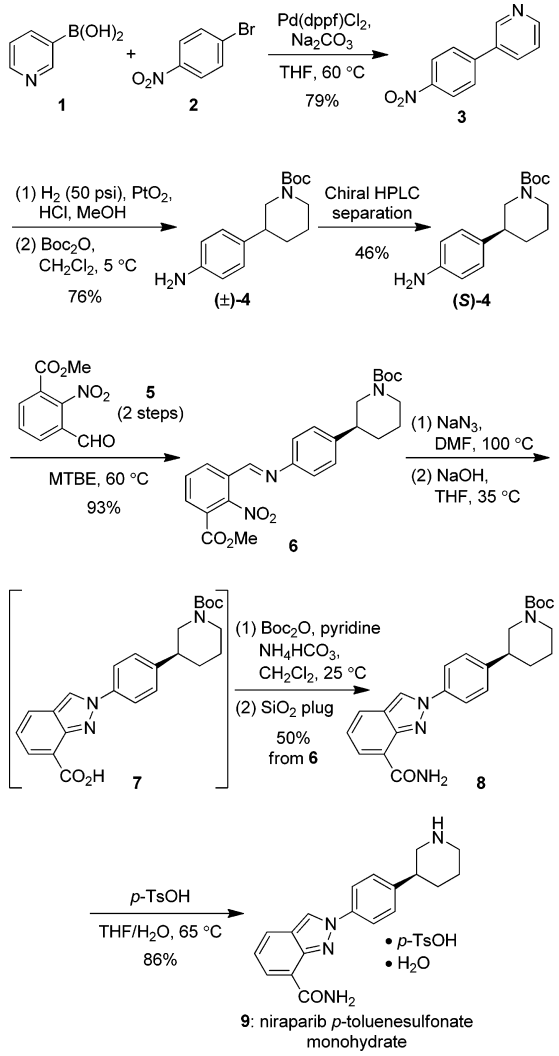


step (Scheme 2). Anticipated to be challenging was controlling the regiochemistry of the coupling to the *N*-2 position, as literature reports of the *N*-arylation of indazoles with aryl halides[5] or aryl boron species[6] suggested a preference for coupling at the undesired *N*-1 position. However, we anticipated that the presence of the C-7 substituent in indazole **11** could offer a handle to modulate the regiochemistry by introducing steric bias. Furthermore, a judicious choice of C-7 substituent could also minimize the number of steps requiring potent compound handling during the manipulation of coupling product **10** to the final API **9**.

**Scheme 2. General retrosynthetic strategy**

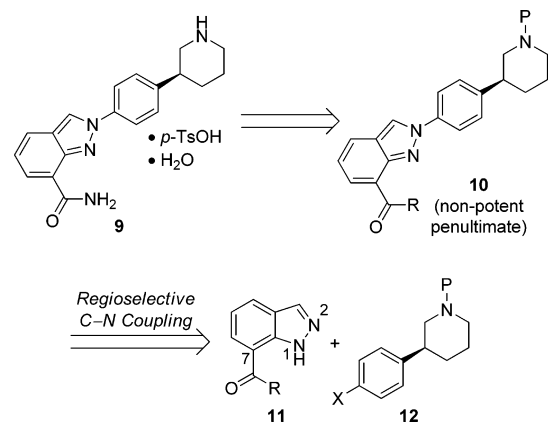


A number of methods have been reported for the asymmetric synthesis of 3-aryl-piperidines.[7] We proposed an approach that would expand the scope of an emerging biocatalytic technology for chiral amine synthesis, namely the use of transaminase enzymes.[8] Starting from racemic open-chain aldehyde **13** (Scheme 3), if selection of the desired (*S*)-aldehyde enantiomer

**Scheme 3. Proposed biocatalytic approach to piperidine 12**

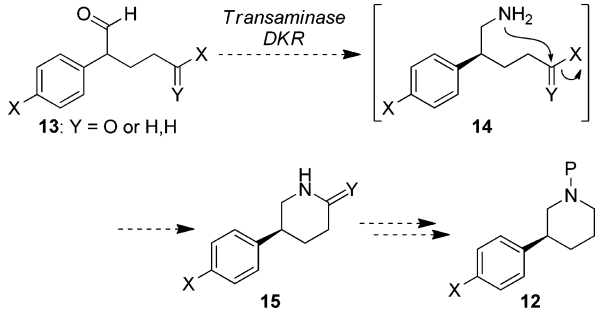


by the transaminase enzyme could be accompanied by racemization of unreacted (*R*)-aldehyde, then a dynamic kinetic resolution (DKR) process would result. This, in theory, could lead to all of the racemic starting material **13** being converted to (*S*)-primary amine **14** with high enantioselectivity. This concept is analogous to the DKR hydrogenation of ketones.[9] Incorporation of a suitably positioned electrophilic group, e.g. an ester or an alkyl halide, into the aldehyde side chain would allow for intramolecular trapping of amine **14** to generate piperidine **15** in a single operation.

At the outset of our work we were encouraged to find that proof of principle of such a transaminase DKR approach had been demonstrated in elegant studies by Kroutil and co-workers, who prepared the five-membered ring lactam 4-phenylpyrrolidin-2-one in up to 92% yield and 68% ee.[10,11] However, to the best of our knowledge, application of this methodology to piperidine homologues has not been reported.

**Enantioselective Synthesis of Piperidine Fragment Using Biocatalysis.** The synthesis of transaminase aldehyde substrate **23** is illustrated in Scheme 4. Friedel–Crafts acylation of bromobenzene with succinic anhydride **16**, using stoichiometric $AlCl_3$ as a promoter, afforded ketoacid **17**.[12] Temperature control during the exothermic quench of the reaction mixture into aqueous HCl was required to minimize formation of the debrominated byproduct **18**; below 35 °C the level of **18** formed was typically 1–2%, and this was easily rejected during downstream crystallizations. The crude product **17** was isolated in 85–90% purity, and contained a number of more nonpolar byproducts. The purity was upgraded to 99% by extraction into aqueous basic solution followed by crystallization upon reacidification, affording acid **17** in 93% overall yield. Acid **17** was then converted to the corresponding isopropyl ester **19** in 93% yield under standard Fisher esterification conditions. After distillative removal of the 2-propanol solvent and aqueous workup, isopropyl ester **19** was crystallized from heptanes in 99% purity and 93% yield. The corresponding methyl (**20**) and ethyl (**21**) ester analogues were prepared in a similar manner, but were found to give much lower yields in subsequent steps.


dx.doi.org/10.1021/op400233z | Org. Process Res. Dev. 2014, 18, 215–227

**Scheme 4. Preparation of aldehyde 23**

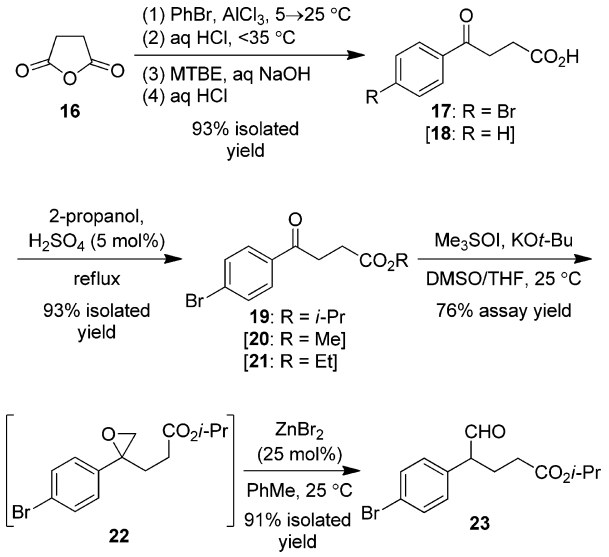


The homologation of ketone **19** to aldehyde **23** was effected using a two-step epoxidation/rearrangement protocol. The epoxidation step was carried out by premixing solid $Me_3SOI$ and KO*t*-Bu in DMSO, followed by the addition of a solution of ketone **19** in 1:1 DMSO/THF. This mixed solvent system represented an appropriate balance between reaction volume efficiency (significantly less solvent volume required to solubilize ketone **19** using THF) and yield (cleaner reaction profile in DMSO). After a 2 h reaction time at room temperature followed by aqueous workup, epoxide **22** was obtained in 76% HPLC assay yield. Identifiable components of the mass balance of this reaction appeared to result from competitive nucleophilic attack at the ester group and/or opening of the epoxide ring. These more polar byproducts were effectively partitioned into the aqueous phase during workup, such that the final organic layer contained epoxide **22** at relatively high purity (~90 HPLC area %). Epoxide **22** was an oil, and could not be crystallized. For evaluation of the rearrangement step, small samples of product were purified by flash chromatography.

Initial attempts at the conversion of epoxide **22** to aldehyde **23** using $BF_3{\cdot}OEt_2$ were not promising, with the reactions being capricious and low-yielding. Screening of conditions was therefore performed using microscale high-throughput experimentation (HTE) techniques.[13] A total of 12 acids and 8 solvents were evaluated in 96-well plate format, and selected results are illustrated in Figure 1. Of the acids screened, $ZnBr_2$ and $InBr_3$ were found to be uniquely effective, with a trend to increasing product formation as solvent polarity decreased. Although the screening results suggested $CH_2Cl_2$ was the solvent of choice, PhMe was preferred for scale up on the basis of cost, with the same consideration driving the selection of $ZnBr_2$ over $InBr_3$ as the Lewis acid promoter. In addition, a higher-boiling solvent was desirable for development of a through process from ketone **19** (vide infra). It was found that the use of a 25 mol % loading of $ZnBr_2$ in PhMe resulted in >99% conversion of epoxide **22** within 1.5 h at room temperature (Scheme 4).[14] After filtration to remove Zn salts, aldehyde **23** could be isolated in 91% yield by flash chromatography.

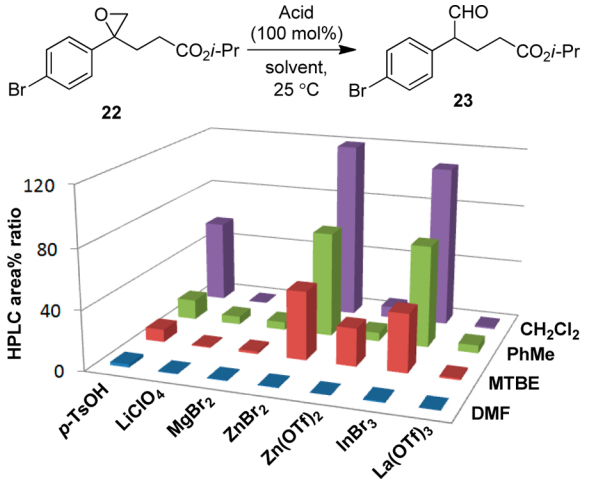


**Figure 1.** Selected results of epoxide rearrangement HTE screening.[15]

Aldehyde **23** was initially screened against a small panel of isolated transaminase enzymes,[16] using pyridoxal-5-phosphate (PLP) as a cofactor and *i*-$PrNH_2$ as the amine donor. As shown in Table 1, ATA-301 was identified as providing good

**Table 1. Results of first-pass transaminase screening of aldehyde 23**

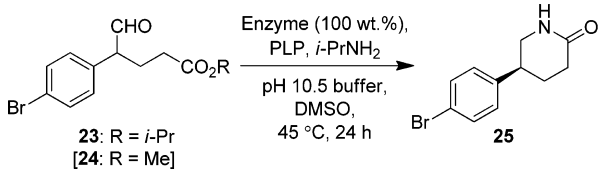


| entry | enzyme | HPLC area % of **25** | ee (%) of **25** |
|---|---|---|---|
| 1 | ATA-007 | 19 | n.d. |
| 2 | ATA-013 | 84 | 75 |
| 3 | ATA-014 | 87 | 59 |
| 4 | ATA-016 | 87 | 66 |
| 5 | ATA-301 | 81 | 99 |
| 6 | ATA-234 | 89 | 0 |
| 7 | CDX-010 | 88 | 44 |
| 8 | CDX-017 | 72 | 45 |

conversion to the desired lactam **25** with excellent enantioselectivity (>99% ee). The use of the corresponding methyl ester **24** generally resulted in worse reaction profiles (due to competing background ester hydrolysis) and lower enantioselectivities, although using ATA-301 lactam **25** was formed in 99% ee and 68 HPLC area%. Based on these initial findings, the use of isopropyl ester **23** with enzyme ATA-301 was selected for further optimization.

During the initial screening, variable levels of formation of ketone **19** (Figure 2) were observed; this was found to result from oxidative degradation of aldehyde starting material **23** under the basic conditions, occurring even in the absence of enzyme. This side reaction could be obviated by rigorous inertion of the vessel under nitrogen. Variation of pH revealed that a pH of 10.5 was the optimum balance between the rate of the desired transaminase reaction and that of competing ester hydrolysis to give acid **26**. Sufficient enzyme stability was maintained at 45 °C to fully consume aldehyde starting material **23** and enable a satisfactory rate of cyclization of amine intermediate **27** (typically less than 2% of **27** remained at the


dx.doi.org/10.1021/op400233z | *Org. Process Res. Dev.* 2014, 18, 215−227

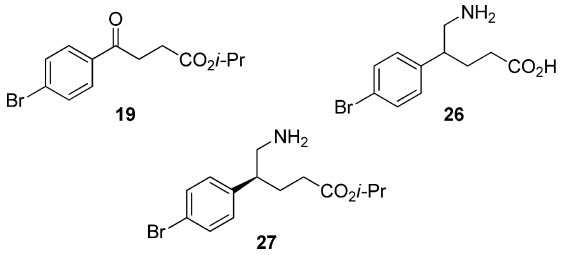


**Figure 2.** Proposed structures of side products **19** and **26**, and intermediate **27** formed during the transaminase reaction.

end of reaction). An acceptable reaction profile could be achieved at a reduced enzyme loading of 50 wt %, albeit at the expense of extended reaction time.

Under these optimized conditions, lactam **25** was formed in 86% assay yield and >99% ee starting from 35 g of isopropyl ester **23** (Scheme 5). Isolation of the product was accomplished with good recovery by aqueous workup followed by crystallization from IPAc.

**Scheme 5. Result of 35-g-scale transaminase reaction of aldehyde 23**

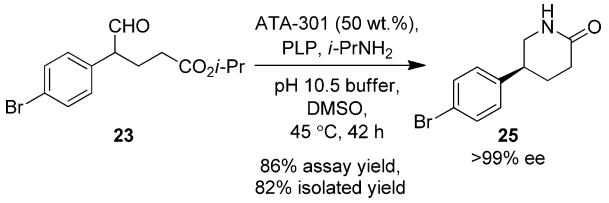


While these results were highly encouraging, there were improvements to be made for development of a practical process. Aldehyde **23** was obtained as a solution in PhMe following the $ZnBr_2$-promoted epoxide rearrangement, but the PhMe would need to be removed prior to the transaminase step due to the incompatibility of the enzyme with common organic solvents. Aldehyde **23** was an oil, precluding its isolation by crystallization, and was also found to have limited stability both when stored neat and in solution. We sought a more stable aldehyde surrogate and hypothesized that the corresponding bisulfite adduct **28** (Scheme 6) could serve this purpose, liberating the parent aldehyde in situ under the basic conditions of the transaminase reaction. As shown in Scheme 6, treatment of the PhMe solution of crude aldehyde **23** with aqueous $NaHSO_3$ resulted in formation and extraction of bisulfite adduct **28** into the aqueous layer.[17] Relative to aldehyde **23**, bisulfite **28** demonstrated improved stability in solution, with a degradation rate of <1% per day at ambient temperature. After a phase cut and wash with heptane, the aqueous layer containing **28** could be charged directly to the transaminase reaction. Performance of bisulfite **28** closely matched that of using the parent aldehyde **23**. In addition, further screening had identified the ATA-302 enzyme as a more robust variant and, under the conditions illustrated in Scheme 6, lactam **25** (>99% ee) was isolated in 84% yield from bisulfite **28**. The 4-step through process from ester **19** to lactam **25** proceeded reliably on 100 g scale. To achieve full conversion of bisulfite **28**, relatively large enzyme loadings (35 wt % relative to starting material **28**) and reaction times (44 h) were required. To support larger-scale production in a pilot-plant setting, optimization of the transaminase enzyme structure to

**Scheme 6. Preparation of C−N coupling substrate 31**

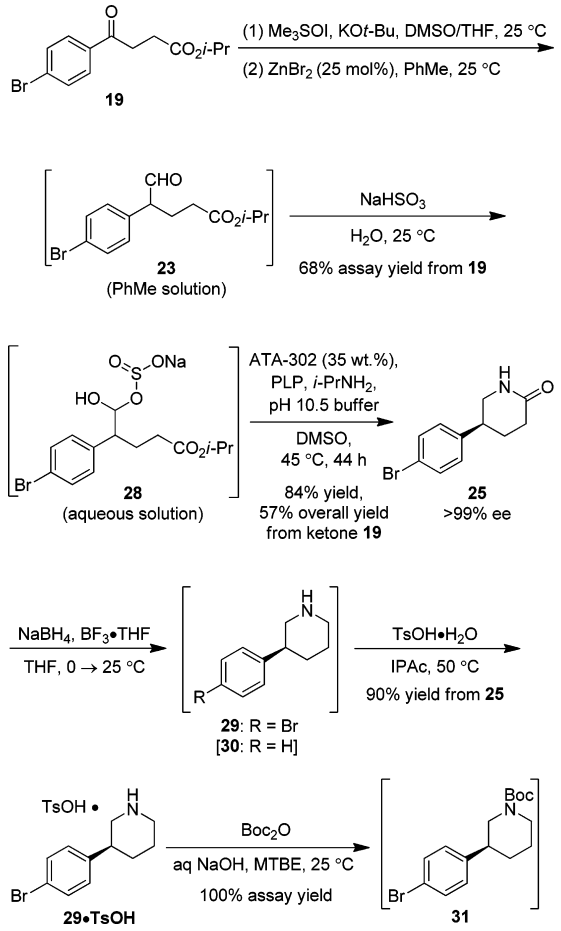


improve activity through rounds of directed evolution[8a] would be warranted.

A number of reducing agents were evaluated for the conversion of lactam **25** to piperidine **29**. DIBAL, Red-Al, or $LiBH_4$ led to product formation but also resulted in varying amounts of des-bromo impurity **30** (Scheme 6). Borane reduction, however, was more efficient and gave minimal debromination. The use of borane generated in situ from $NaBH_4$ and $BF_3$·THF was preferred over commercially available borane solutions for cost, reagent handling, and volume productivity reasons.[18,19] Initially, an elevated reaction temperature of 55 °C was required to obtain full conversion and a clean profile. Subsequent optimization studies revealed that the addition of EtOH (3 equiv relative to lactam **25**, 1 equiv relative to $NaBH_4$) allowed the reaction to proceed at ambient temperature. Hazard evaluation of this reduction was performed due to three potential safety issues, namely: (1) potential for thermal hazards, (2) corrosion of glass-lined equipment due to the formation of HF, and (3) generation of diborane, a highly toxic and explosive gas. No potential thermal hazards were identified by DSC screening, and a paper assessment of the chemistry suggested that generation of more than trace amounts of fluoride ion was not expected. Monitoring of the vessel headspace of a trial reaction by FTIR spectroscopy showed that the level of diborane gas generated was significantly below the lower explosive limit in air (8400 ppm) at all stages during the process (Figure 3).[20]

The piperidine product **29** from the reduction was only weakly crystalline and was difficult to isolate as a solid with


dx.doi.org/10.1021/op400233z | Org. Process Res. Dev. 2014, 18, 215−227

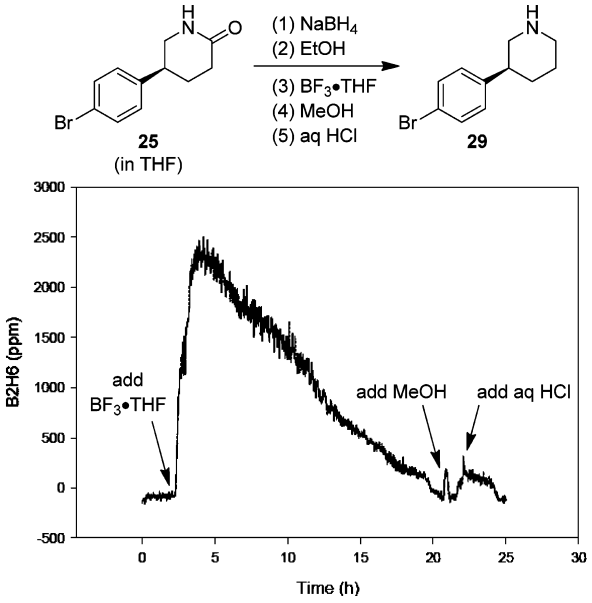


**Figure 3.** Time course of diborane levels in vessel headspace monitored by FTIR spectroscopy.

good reproducibility; therefore it was converted to the corresponding *p*-toluenesulfonate salt **29·TsOH** (Scheme 6), affording good physical properties and impurity control (isolated solids were >99 wt % purity). The subsequent Boc protection to give C−N coupling substrate **31** was achieved in quantitative yield using $Boc_2O$ in a biphasic mixture of MTBE and aqueous NaOH. The product **31** was a low-melting, waxy solid that was difficult to handle; thus, it was more convenient to carry forward the crude product solution (following a solvent-switch into DMAc, vide infra) into the C−N coupling step. The synthesis of compound **31** was thus accomplished in nine steps (four isolations) and 44% overall yield from commercial starting materials.

**Alternative Biocatalytic Routes to Piperidine Fragment.** In addition to approach described above, proof-of-concept was also established on a second transaminase DKR-based route in which lactol **35** (Scheme 7) was employed as an alternative aldehyde surrogate. Lactone **34** was prepared in two steps with minor adjustments to a procedure reported previously from these laboratories.[21] Dianion formation from acid **32** using MeLi or LDA (rather than *n*-HexLi, to avoid undesired metal−halogen exchange) followed by addition of 1-bromo-3-chloropropane gave crude monoalkylated product **33**, which could be cyclized by treatment with DBU in IPAc (cleaner reaction than in THF). On laboratory scale, lactone **34** was isolated by flash chromatography, although the overall yield for the two-step process was somewhat variable (60−80%). Reduction of lactone **34** to lactol **35** was effected using 1 equiv of DIBAL in 1:1 THF/PhMe at −15 °C. The use of THF cosolvent was required to maintain complete solubility of the lactone starting material **34** below ambient temperature. An excess of DIBAL or higher temperatures led to overreduction to the diol. After aqueous workup, lactol **35** was isolated as a stable solid in 89% yield by crystallization from PhMe/heptane.

Lactol **35** proved to be an excellent substrate for transaminase DKR. Little modification was needed to the reaction conditions that had been developed for aldehyde **23**, with the primary amine product **36** being generated in >98% ee and >99% HPLC area% purity at full conversion of the starting

**Scheme 7. Lactol transaminase route to piperidine 31**

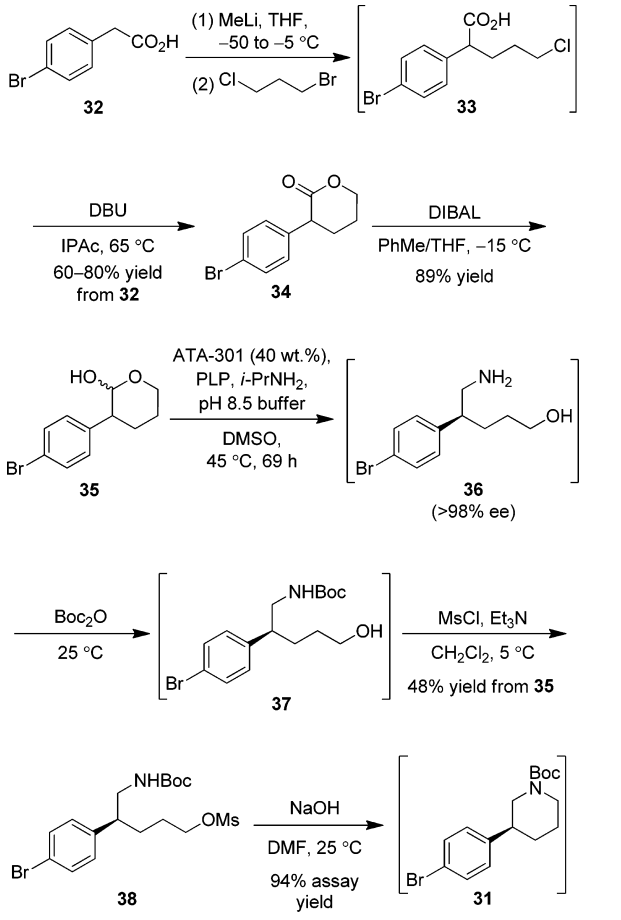


material **35** (Scheme 7). The main procedural change was that the optimum pH for this process was 8.5 rather than 10.5; possibly at lower pH there is a higher concentration of the open-chain aldehyde available in equilibrium. The amino alcohol product **36** had high water solubility, and attempted recovery by extraction with organic solvents resulted in significant product loss to the aqueous phase. The workup was therefore changed to precipitate the spent enzyme at the end of the reaction using aqueous HCl, followed by removal by filtration. The acidic filtrate was then adjusted to pH 10 and treated directly with $Boc_2O$ to give alcohol **37**, which could be readily extracted. This crude product was, in turn, reacted with MsCl in the presence of $Et_3N$ to give mesylate **38**, which could be crystallized from hexanes/EtOAc. Mesylate **38** was isolated in >99% purity and 48% overall yield for this three-step sequence. HTE screening of the intramolecular cyclization of mesylate **38** revealed that stronger bases were more effective (Figure 4); confirmation of representative conditions (NaOH, DMF) gave Boc-piperidine **31** in 94% assay yield (Scheme 7).

Although less extensively developed than the approach using bisulfite adduct **28**, this lactol transaminase route offers a viable alternative. The use of chloroaldehyde **39** or the corresponding bisulfite adduct **40** as substrates was also briefly explored, as these were expected to give piperidine **29** directly from the transaminase DKR process (Scheme 8). In practice, however, both the synthesis of the substrates and their performance in the transaminase reaction were plagued by low yields and instability issues, and this approach was not pursued at length.


dx.doi.org/10.1021/op400233z | Org. Process Res. Dev. 2014, 18, 215−227

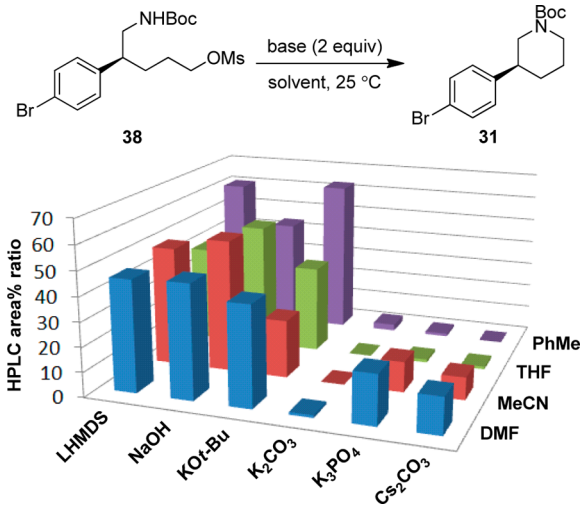


**Figure 4.** Screening results of the intramolecular cyclization of mesylate **38**.[15]

**Scheme 8. Alkyl chloride transaminase approach**

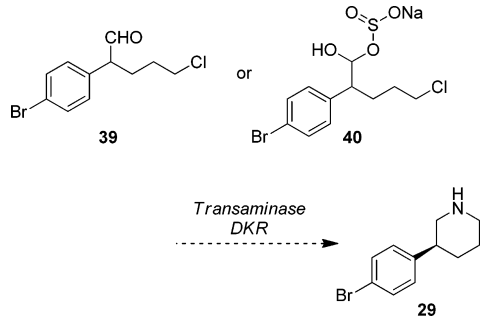


**C–N Coupling.** With bromide **31** in hand, a regioselective C–N coupling with the indazole heterocycle was required to efficiently assemble the tetracyclic core of the target API. Copper ligand catalysis[5] was first evaluated using a series of indazoles **41**–**46** (Table 2) that were either commercially available or readily prepared in one step from carboxylic acid **41**. Key results from the output of several hundred microscale screening experiments are summarized in Table 2 and Figure 5.

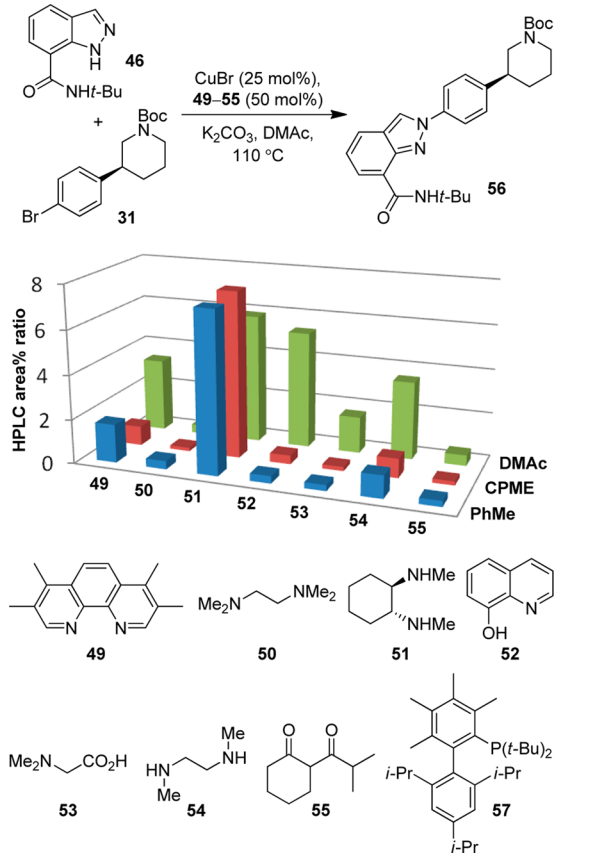


**Figure 5.** Selected ligand screening results of C–N coupling of indazole **46**.[15]

**Table 2. Regioselectivity of C–N coupling with indazoles 41–46**

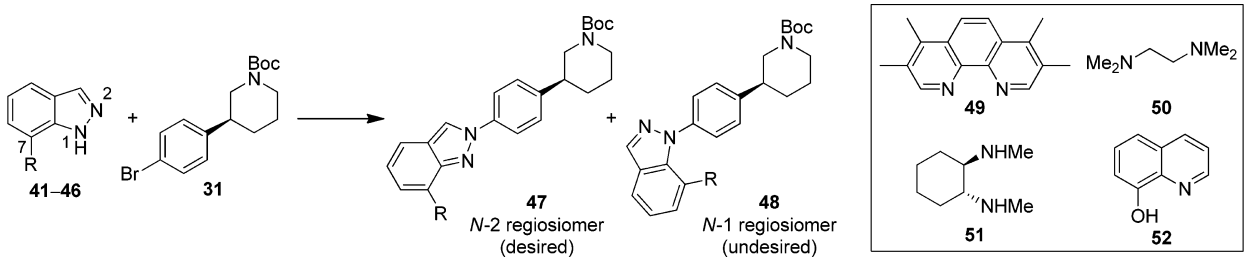


| Entry | Indazole | R | Conditions[a] | Conversion[b] | Regioselectivity *N*-2:*N*-1 (**47**:**48**) |
|---|---|---|---|---|---|
| 1 | **41** | $CO_2H$ | CuI (10 mol%), $FeCl_3$•$6H_2O$ (20 mol%), **49** (20 mol%), $K_3PO_4$, DMSO, 110 °C | 33 | 1:1 |
| 2 | **42** | $CO_2Me$ | CuI (13 mol%), **50** (24 mol%), $K_3PO_4$, DMSO, 125 °C | 61[c] | 1:1 |
| 3 | **43** | CN | CuBr (25 mol%), **51** (50 mol%), $K_2CO_3$, NMP, 110 °C | 96 | 17:1 |
| 4 | **44** | $CO_2t$-Bu | CuBr (25 mol%), **52** (50 mol%), $K_3PO_4$, DMI,[d] 110 °C | 87 | 33:1 |
| 5 | **45** | CONH*t*-Bu | CuBr (25 mol%), **51** (50 mol%), $K_2CO_3$, PhMe, 110 °C | 94 | > 50:1 |
| 6 | **46** | 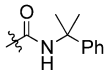 | CuBr (25 mol%), **51** (50 mol%), $K_2CO_3$, PhMe, 110 °C | 90 | > 50:1 |

[a]All reactions were run for 24 h. [b]Conversion of bromide starting material **31** was measured by HPLC. [c]Significant competing ester hydrolysis was observed. [d]DMI = 1,3,dimethyl-2-imidazolidinone.


dx.doi.org/10.1021/op400233z | *Org. Process Res. Dev.* 2014, 18, 215–227

**Scheme 9. Optimized C−N coupling of Boc-protected piperidine 31 with indazole 46**

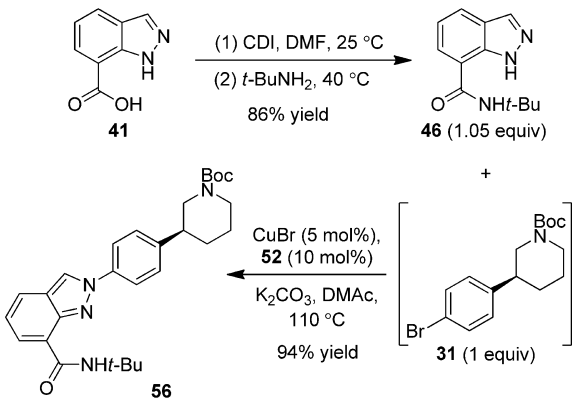


The carboxylic acid (**41**) and methyl ester (**42**) indazole derivatives displayed no regioselectivity (Table 2, entries 1 and 2), while higher selectivity for arylation at the desired *N*-2 position was observed with indazoles **43**−**46** (entries 3−6). The good regioselectivity observed using cyano-substituted indazole **43** (entry 3) confounds a simplistic analysis that steric bulk at the C-7 position on the indazole ring is the sole determining factor. In addition to their excellent regioselectivity, both amide derivatives **45** and **46** were appealing in that they offered a more streamlined endgame to the API; no late-stage amidation step would be required, and their corresponding C−N coupling products **47** (penultimate to the API) were determined to not require potent compound handling conditions. Ultimately, the *tert*-butylamide **45** was selected over the cumyl derivative **46** on the basis of atom-economy and raw material cost.

The performance of the Cu-catalyzed C−N coupling was found to be dependent on a number of parameters. The choice of ligand was critical. Although diamine **51** was effective under a broad range of screening conditions (Figure 5), 8-hydroxyquinoline **52**[22] was competitive using the specific conditions of $K_2CO_3$ as base in DMAc. Both ligands gave very high levels of regioselectivity (>100:1) and chemoselectivity (no coupling at the amide nitrogen was observed). The ligands were differentiated on cost (8-hydroxyquinoline **52** being cheaper) and subsequent catalyst loading studies, which showed that the coupling yield dropped precipitously as the amount of diamine ligand **51** was lowered from 40 mol % relative to aryl bromide **31**, while systems using 8-hydroxyquinoline **52** were more robust. Reaction temperatures above 100 °C were required to achieve full conversion of aryl bromide **31**. CuBr was the optimum copper source, with CuI or $Cu_2O$ being much less efficient. The optimum ligand:Cu ratio was 2:1. Mixing CuBr and 8-hydroxyquinoline **52** in DMAc resulted in formation of a homogeneous solution which was stable for at least 18 h prior to addition of the substrates. However, preforming the catalyst was not a requirement, and it was found to be operationally easier to simply add all the reaction components sequentially to the vessel. Indeed, a Cu(II)/bis(8-hydroxyquinoline) complex is commercially available but was not as effective as using the species generated in situ from CuBr and ligand **52**. The reaction was tolerant to the presence of at least 10% (by volume) water but was found to be highly oxygen sensitive; intrusion of oxygen resulted in stalling of the reaction and degradation of unreacted indazole **46**. To obtain consistent results, degassing of the reaction mixture prior to heating,

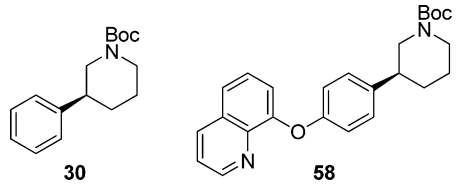


**Figure 6.** Byproducts formed during the C−N coupling.

**Scheme 10. C−N coupling of indazole 46 with unprotected piperidine 29·TsOH**

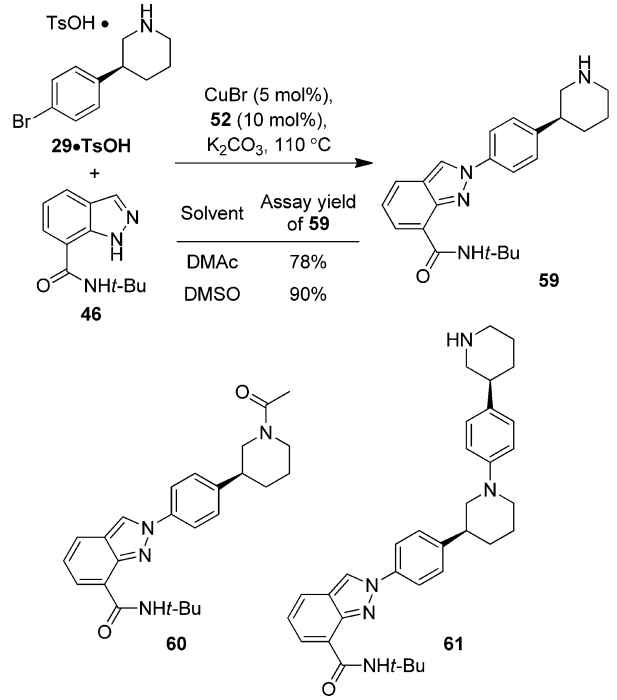


followed by a nitrogen sweep through the vessel headspace during the reaction, was performed. The reaction is heterogeneous, as the $K_2CO_3$ base does not fully dissolve. On laboratory scale with overhead mechanical stirring, powdered and granular $K_2CO_3$ were found to be equally effective. Palladium catalysis of the C−N coupling was also screened, but only the expensive, sterically hindered phosphine ligand **57**[23] (Figure 5) gave good conversion, accompanied by an impurity profile inferior to that of the Cu-catalyzed reactions.

The optimized C−N coupling sequence is illustrated in Scheme 9. Indazole **46** was prepared from acid **41** and *tert*-butylamine through a CDI-mediated amide bond formation, which proved superior to mixed-anhydride or HATU amidation protocols. Removal of the $CO_2$ (by sparging or applying vacuum) generated during the acyl imidazole activation step facilitated the subsequent displacement by *tert*-butylamine. A slight excess of CDI was used (1.2 equiv), although significant overcharge beyond this was found to lead to formation of elevated levels of 1,3-di-*tert*-butylurea, which could not be efficiently rejected during the crystallization of indazole **46** by addition of water to the reaction mixture.

Under the optimized conditions shown in Scheme 9, coupling of bromide **31** in DMAc with a near stoichiometric amount of indazole **46** at 5 mol % copper loading proceeded to >99% conversion within 24 h. The observed regioselectivity was >200:1 for the *N*-2 isomer **56**. Minor byproducts identified in the mixture were debrominated piperidine **30** and


dx.doi.org/10.1021/op400233z | Org. Process Res. Dev. 2014, 18, 215−227

compound **58** (Figure 6), the latter resulting from C−O coupling between ligand **52** and the aryl bromide **31**. After filtration to remove inorganic salts (filtration rate was improved by the addition of Celite), the desired product **56** could be directly crystallized by addition of aqueous solution. The use of 10% aqueous citric acid afforded slightly improved copper removal compared to pure water or aqueous ammonia, with lower copper levels being retained in the product cake (<100 ppm vs 300−500 ppm). Compound **56** was isolated in 94% yield and >99% weight % purity.

Proof-of-concept was also demonstrated on the use of piperidine tosylate salt **29·TsOH** in the C−N coupling. When tosylate salt **29·TsOH** was subjected to the conditions that had been optimized for the corresponding Boc-protected substrate **31**, product **59** was formed in a lower assay yield of 78% (Scheme 10), with acetyl derivative **60** and homocoupling adduct **61** being major byproducts. A small screening study identified DMSO as a solvent that gave an improved reaction profile, generating the desired product **59** in 90% assay yield. In addition to 8-hydroxyquinoline **52**, ligands **51** and **53** were also effective. Given the potential for energetic decomposition of DMSO,[24] accelerating rate calorimetry was used to confirm that there were no thermal safety issues with running a process under these conditions. Although not optimized further, this coupling approach would allow a more expedient route to the API by eliminating the Boc protection step.

**Deprotection and API Isolation.** Removal of both the *tert*-butyl amide and piperidine-Boc protecting groups from penultimate **56** could be accomplished in a single step under strongly acidic conditions (Scheme 11). While the Boc group was cleaved readily, more forcing conditions were required to fully liberate the primary amide. Treatment of penultimate **56** with neat anhydrous methanesulfonic acid (MSA, 22 equiv) at 40 °C resulted in 98% conversion to the MSA salt of the API (**9·MSA**) within 1 h. However, deprotection of the remaining 2% of *tert*-butylamide intermediate **59·MSA** slowed dramatically, and required more than 24 h to reach full conversion. It was found that use of an aromatic cosolvent to scavenge *tert*-butyl cations significantly enhanced the reaction rate. Of a small selection of solvents evaluated, *ortho*-xylene was the most effective. In practice, when a slurry of penultimate **56** in *o*-xylene was treated with excess MSA at 40 °C, formation of **9·MSA** with <0.1% *tert*-butylamide **59·MSA** remaining was achieved within 3 h.

**Scheme 11. Conversion of penultimate 56 to API 9**

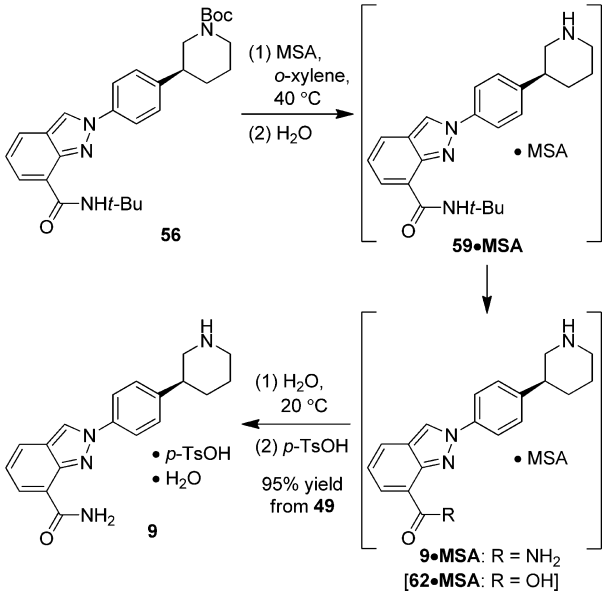


Isolation of the API was facilitated by exploiting the large difference in aqueous solubility between the desired *p*-toluenesulfonate salt monohydrate crystalline form **9** (<1 mg/mL) and that of the mesylate salt **9·MSA** resulting from the deprotection reaction (>100 mg/mL). Once the deprotection was complete, mesylate salt **9·MSA** was partitioned into an aqueous layer by dilution with water, and the organic phase was cut away. Control of the batch temperature below 25 °C during the water addition was required to minimize hydrolysis of the primary amide group to give undesired carboxylic acid **62·MSA**. Addition of an aqueous solution of *p*-TsOH then resulted in salt metathesis and solubility-driven crystallization to afford the desired salt polymorph **9** in 95% yield. This material was isolated in excellent purity (99.8 HPLC area%, >99.7% ee) and met all the required specifications.

## CONCLUSION

In summary, two new synthetic routes to the PARP inhibitor niraparib (**9**) have been developed which feature novel bio- and chemocatalytic transformations (Scheme 12). The scope of biocatalytic transaminase reactions has been expanded to encompass highly efficient and stereoselective dynamic kinetic resolution processes using a bisulfite adduct or lactol as a more stable aldehyde surrogate. Incorporation of appropriate functional group handles into the transaminase reaction substrates enabled a concise, enantioselective synthesis of the 3-arylpiperidine ring system. Convergent fragment coupling was achieved through a copper-catalyzed C−N arylation with an indazole derivative that proceeded with high chemo- and regioselectivity. Development of these and other steps was facilitated by extensive use of microscale high-throughput experimentation techniques, which significantly expanded the parameter space for reaction screening while concomitantly reducing the time, resources and material needed for hit-finding and optimization.

The route using bisulfite adduct **28** comprises 12 steps with 7 isolations, and proceeds in 40% overall yield for the longest linear sequence of 11 steps. The approach using lactol **35** was less extensively developed, but proceeds in 23−30% overall yield for the longest linear sequence of 9 steps, comparing favorably with the 11% overall yield of the first kilogram-scale synthesis. In both of these new routes, several reactions could be telescoped to reduce cycle time and the number of isolations, and potent compound handling operations were minimized by developing a streamlined process from penultimate **56** in which the final API could be isolated by using a salt metathesis-driven crystallization. While scope for further optimization exists, both routes address key issues hindering further scale-up of the previously described syntheses of niraparib (**9**). They would also be expected to have greatly reduced cost and environmental impact, and further demonstrate the enabling potential of continuing advances in catalysis technology on chemical process development.

## EXPERIMENTAL SECTION

**General.** All reactions were carried out under $N_2$ atmosphere. THF was dried by storing over molecular sieves.


dx.doi.org/10.1021/op400233z | Org. Process Res. Dev. 2014, 18, 215−227

**Scheme 12. Summary of new routes to niraparib 9**

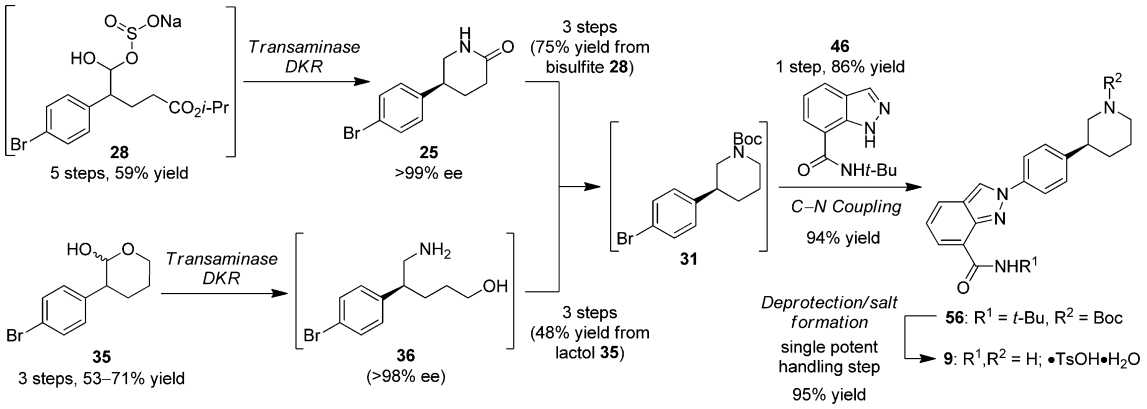


All other commercial chemicals were used as received. Temperatures refer to internal batch temperatures, unless otherwise stated. Reactions were monitored by reverse-phase HPLC on a Hewlett-Packard 1100 Series instrument, using the following conditions as a standard method - Column: Ascentis Express C18 column (100 mm × 4.6 mm, 2.7 $\mu$m fused-core particle size); Eluent: (A) 0.1% aq $H_3PO_4$, (B) MeCN; Gradient: linear ramp from 10% to 95% B over 6 min, then hold at 95% B for 2 min, then 2 min post time at 10% B; Flow rate: 1.8 mL/min; Sample injection volume: 5 $\mu$L; Column temperature: 40 °C; UV detection: 210 nm. HPLC assay yields and weight % purities were obtained using analytical standards of known purity. $^1$H and $^{13}$C NMR spectra were recorded on Bruker Avance NMR Spectrometers. Chemical shifts are reported in ppm relative to the residual deuterated solvent. Melting points were obtained on a Büchi B-545 Melting Point instrument and are uncorrected. Optical rotations were measured on a Perkin-Elmer 241 polarimeter, and data are reported as $[\alpha]^{20}_D$ (concentration in g/100 mL, solvent). Infrared spectra were recorded as thin films on a Nicolet Nexus 570 FT-IR instrument. High-resolution mass spectra were recorded on a Micromass QTOF Ultima API US mass spectrometer by electrospray ionization.

**4-(4-Bromophenyl)-4-oxobutanoic Acid (17).** Bromobenzene (695 mL, 6.6 mol) and succinic anhydride **16** (110 g, 1.1 mol) were combined at 20−25 °C, and slurry was cooled to 2−5 °C. $AlCl_3$ (293 g, 2.2 mol) was added in one portion, and after 30 min the slurry was allowed to warm to 25 °C over 5 h, and then aged at that temperature for a further 80 h. The HCl evolved during the reaction was vented with a gentle $N_2$ sweep through the vessel headspace into a NaOH scrubber. A separate vessel was charged with water (1.2 L) and 37% aq HCl (220 mL) and the solution cooled to 0−5 °C. The Friedel−Crafts reaction mixture was then transferred over a period of 30 min into the stirred HCl solution (**EXOTHERMIC**), maintaining the temperature of the quenched mixture below 35 °C. The resulting white slurry was aged at 10 °C for 1 h, and was then filtered and the cake washed with water (2 × 800 mL). The product wet cake was then slurried in MTBE (500 mL), and aq NaOH (200 mL 10 M aq NaOH dissolved in 1 L water) was added over 5 min at 20−25 °C. After a further 15 min the layers were separated. The aqueous layer was acidified to pH 1 using 37% aq HCl (~250 mL) at 20−25 °C. The resulting slurry was aged at 10 °C for a further 1 h and then filtered. The cake was washed with water (2 × 500 mL), then dried in vacuo under a $N_2$ sweep at 20−25 °C for 4 h then at 50 °C for 16 h to give 265 g of **17** (99 wt %, 93% corrected yield) as a white powder. Mp 147 °C; HPLC $t_R$ 3.47 min; $^1$H NMR (400 MHz, DMSO-$d_6$) $\delta$ 12.15 (s, 1H), 7.93−7.89 (m, 2H), 7.76−7.72 (m, 2H), 3.23 (t, $J$ = 6.5 Hz, 2H), 2.58 (t, $J$ = 6.5 Hz, 2H); $^{13}$C NMR (101 MHz, DMSO-$d_6$) $\delta$ 197.7, 173.7, 135.4, 131.8, 129.9, 127.2, 33.1, 27.8; IR (neat) 2893, 1694, 1670, 1583, 1408, 1197, 839, 790, 645 cm$^{-1}$; HRMS calcd for $C_{10}H_{10}BrO_3$ $[M + H]^+$ 256.9813, found 256.9818.

**Isopropyl 4-(4-Bromophenyl)-4-oxobutanoate (19).** Concentrated $H_2SO_4$ (2.13 mL, 39.9 mmol) was charged to a slurry of acid **17** (205 g, 797 mmol) in 2-propanol (4 L) at 20 − 25 °C, and the mixture was heated to gentle reflux (82−83 °C). After 40 h the solution was cooled, and then concentrated to a volume of 350−400 mL at 35−40 °C. The resulting slurry was dissolved in MTBE (1.2 L), and aq $Na_2CO_3$ (prepared by dissolving 35 g $Na_2CO_3$ in 500 mL water) was added in one portion at 20−25 °C, and the biphasic mixture was stirred for 10 min. The layers were separated, and the organic layer was washed with water (1 × 400 mL) and filtered. The filtrate was concentrated and solvent-switched by distillation under vacuum at 35−40 °C (bath temperature) into heptane to a final volume of ~600 mL. The resulting slurry was aged at 20−25 °C for 4 h, then at 2−5 °C for a further 1 h. Filtration, washing with chilled (~5 °C) heptane (1 × 200 mL), and drying in vacuo at 20−25 °C under a $N_2$ sweep for 16 h afforded 224 g of **19** (99 wt %, 93% corrected yield) as a white powder. Mp 62 °C; HPLC $t_R$ 5.17 min; $^1$H NMR (400 MHz, $CDCl_3$) $\delta$ 7.85−7.81 (m, 2H), 7.60−7.57 (m, 2H), 5.01 (sept, $J$ = 6.5 Hz, 1H), 3.24 (t, $J$ = 6.5 Hz, 2H), 2.71 (t, $J$ = 6.5 Hz, 2H), 1.23 (d, $J$ = 6.5 Hz, 6H); $^{13}$C NMR (101 MHz, $CDCl_3$) $\delta$ 197.1, 172.1, 135.3, 131.8, 129.5, 128.2, 68.0, 33.3, 28.5, 21.7; IR (neat) 2980, 2917, 1721, 1679, 1582, 1310, 1170, 1115, 784 cm$^{-1}$; HRMS calcd for $C_{13}H_{16}BrO_3$ $[M + H]^+$ 299.0283, found 299.0283.

**Isopropyl 3-(2-(4-Bromophenyl)oxiran-2-yl)-propanoate (22).** Trimethylsulfoxonium iodide (230 g, 1.04 mol) was slurried in DMSO (300 mL) at 20−25 °C. KO*t*-Bu (113 g, 1.01 mol) was added in one portion, followed by additional DMSO (300 mL). After 1.5 h a solution of ketone **19** (223 g, 0.75 mmol) in a mixture of THF (250 mL) and DMSO (150 mL) was added over 45 min at 20−25 °C. After a further 2 h the reaction was diluted with hexanes (1 L), then quenched by the addition of chilled (~5 °C) water (600 mL) over 5 min, maintaining the temperature below 25 °C. The layers were separated, and the organic layer was washed with water (1 × 500 mL) and then sat. aq NaCl (1 × 500 mL). HPLC assay gave 176 g (76% yield) of epoxide **22** in the final


dx.doi.org/10.1021/op400233z | Org. Process Res. Dev. 2014, 18, 215−227

organic solution, which was held overnight at 20−25 °C before being used in the rearrangement step. For characterization, a sample of epoxide **22** was isolated by flash column chromatography on silica gel (gradient elution from 19:1 to 9:1 *n*-hexane/EtOAc), affording a light-yellow oil. HPLC $t_R$ 5.53 min; $^1$H NMR (500 MHz, $CDCl_3$) $\delta$ 7.48−7.46 (m, 2H), 7.27−7.24 (m, 2H), 4.97 (sept, $J$ = 6.5 Hz, 1H), 2.99 (d, $J$ = 5.0 Hz, 1H), 2.71 (d, $J$ = 5.0 Hz, 1H), 2.52 (ddd, $J$ = 14.5, 10.0, 6.0 Hz, 1H), 2.36 (ddd, $J$ = 16.0, 10.0, 6.0 Hz, 1H), 2.26 (ddd, $J$ = 16.0, 10.0, 6.0 Hz, 1H), 2.05 (ddd, $J$ = 14.5, 10.0, 6.0 Hz, 1H), 1.21 (d, $J$ = 6.5 Hz, 3H), 1.20 (d, $J$ = 6.5 Hz, 3H); $^{13}$C NMR (126 MHz, $CDCl_3$) $\delta$ 172.3, 138.4, 131.6, 127.7, 121.6, 67.9, 59.1, 55.5, 30.3, 29.9, 21.7, 21.7; IR (neat) 2978, 2933, 1724, 1179, 1106, 1077, 1009, 820 cm$^{-1}$; HRMS calcd for $C_{14}H_{18}BrO_3$ $[M + H]^+$ 313.0439, found 313.0451.

**Isopropyl 4-(4-Bromophenyl)-5-oxopentanoate (23).** The crude solution of epoxide **22** (HPLC assay 59.5 g **22**, 190 mmol) was solvent-switched by distillation under vacuum at 35−40 °C (bath temperature) into toluene to a final volume of ∼450 mL. Anhydrous $ZnBr_2$ (10.7 g, 47.5 mmol) was added in one portion at 22 °C. The batch warmed from 22 to 30 °C over 30 min (no external cooling was applied). After 1.5 h the slurry (batch temperature 22 °C) was filtered, and the filtrate was washed with 10% aq NaCl (1 × 130 mL). For characterization, a sample of aldehyde **23** was isolated by flash column chromatography on silica gel (gradient elution from 19:1 to 4:1 *n*-hexane/EtOAc), affording a yellow oil. HPLC $t_R$ 5.3 min; $^1$H NMR (500 MHz, $CDCl_3$) $\delta$ 9.67 (d, $J$ = 1.5 Hz, 1H), 7.53−7.51 (m, 2H), 7.08−7.05 (m, 2H), 4.99 (sept, $J$ = 6.5 Hz, 1H), 3.61 (ddd, $J$ = 8.0, 6.5, 1.5 Hz, 1H), 2.43−2.36 (m, 1H), 2.30−2.18 (m, 2H), 2.02−1.95 (m, 1H), 1.23 (d, $J$ = 6.5 Hz, 3H), 1.21 (d, $J$ = 6.5 Hz, 3H); $^{13}$C NMR (126 MHz, $CDCl_3$) $\delta$ 199.3, 172.2, 134.5, 132.4, 130.6, 122.0, 67.9, 57.4, 31.6, 24.8, 21.8, 21.8.

**(*S*)-5-(4-Bromophenyl)piperidin-2-one (25).** Pyridoxal-5-phosphate (1.51 g, 6.1 mmol) was dissolved in 0.2 M aq borate buffer (487 mL) containing 1 M aq *i*-$PrNH_2$ was added at 20−25 °C. To the resulting solution (pH 10.5) was charged ATA-302 enzyme (56 g) with gentle agitation. Once the enzyme had fully wetted, DMSO (81 mL) was added, and the mixture heated to 45 °C. 923.9 g of a 17.2 wt % bisulfite adduct solution ($^1$H NMR assay 158.9 g **28**, 380.1 mmol) was charged over 3 h. During the addition, and subsequent reaction, the pH of the mixture was maintained at 10.5 by addition of 8 M aq *i*-$PrNH_2$. The reaction was aged for 44 h before being cooled to 30 °C and extracted with a mixture of 3:2 v/v 2-propanol/IPAc (1 × 500 mL). The aqueous layer was back-extracted with a mixture of 3:7 2-propanol/IPAc (1 × 500 mL). The combined organic layers were washed with sat. aq NaCl (2 × 300 mL). The resulting organic layer, containing 85 g of piperidinone **28** (by HPLC assay) at 99.3% ee (SFC assay), was filtered, and the filtrate was concentrated and solvent-switched by distillation under vacuum at 35−40 °C (bath temperature) into IPAc to a final volume of ∼200 mL. The resulting slurry was aged at 20−25 °C overnight, then between −5 and 0 °C for 1.5 h. Filtration, washing with chilled (∼5 °C) IPAc (2 × 40 mL), and drying in vacuo at 20−25 °C under a $N_2$ sweep for 16 h afforded 84 g of **25** (97.5 wt %, 84% corrected yield) as a white powder. Mp 207−207.5 °C; HPLC $t_R$ 3.54 min; $[\alpha]^{25}_D$ +51.9 (*c* 1.38, $CHCl_3$); $^1$H NMR (400 MHz, $CDCl_3$) $\delta$ 7.48−7.45 (m, 2H), 7.14−7.12 (m, 2H), 6.48 (br s, 1H), 3.51−3.46 (m, 1H), 3.34 (t, $J$ = 11.0, 11.0 Hz, 1H), 3.07−2.99 (m, 1H), 2.57−2.44 (m, 2H), 2.12−1.97 (m, 2H); $^{13}$C NMR (101 MHz, $CDCl_3$) $\delta$ 171.7, 140.7, 131.9, 128.7, 120.9, 48.4, 39.0, 31.1, 27.7; IR (neat) 3305, 2950, 2885, 1658, 1612, 1488, 1463, 819, 752 cm$^{-1}$; HRMS calcd for $C_{11}H_{13}BrNO$ $[M + H]^+$ 254.0181, found 254.0191.

**Sodium 2-(4-Bromophenyl)-1-hydroxy-5-isopropoxy-5-oxopentyl sulfite (28).** To the toluene solution of aldehyde **23** was charged a solution of $NaHSO_3$ (24.7 g, 238 mmol) in water (140 mL) in one portion at 20−25 °C, and the biphasic mixture was stirred vigorously for 3 h. The layers were separated, and the aqueous layer washed with heptanes (1 × 60 mL). The aqueous layer (234.2 g) contained 71.2 g bisulfite adduct **28** (30.4 wt % solution, 90% yield from epoxide **22**) by $^1$H NMR assay against a water-soluble internal standard (3-(trimethylsilyl)-1-propanesulfonic acid sodium salt). This solution was held overnight at 20−25 °C before being used in the transaminase step. For characterization, a sample of bisulfite adduct **28** was prepared using an alternative procedure as described in the Supporting Information, affording a white powder as a 1:1 mixture of diastereoisomers. Mp 133−135 °C; HPLC $t_R$ 3.51/3.57 min; $^1$H NMR (400 MHz, $D_2O$) $\delta$ 7.51 (d, $J$ = 8.5 Hz, 2H), 7.49 (d, $J$ = 8.5 Hz, 2H), 7.25 (d, $J$ = 8.5 Hz, 2H), 7.24 (d, $J$ = 8.5 Hz, 2H), 4.84 (sept, $J$ = 6.5 Hz, 1H), 4.83 (sept, $J$ = 6.5 Hz, 1H), 4.66 (d, $J$ = 7.0 Hz, 1H), 4.58 (d, $J$ = 5.5 Hz, 1H), 3.25−3.16 (m, 2H), 2.53−2.46 (m, 1H), 2.44−2.36 (m, 1H), 2.20−1.97 (m, 6H), 1.18 (d, $J$ = 6.5 Hz, 3H), 1.18 (d, $J$ = 6.5 Hz, 3H), 1.15 (d, $J$ = 6.5 Hz, 3H), 1.14 (d, $J$ = 6.5 Hz, 3H); $^{13}$C NMR (101 MHz, $D_2O$) $\delta$ 175.5, 175.3, 140.1, 138.7, 131.5, 131.3, 131.1, 130.5, 120.4, 86.9, 86.3, 69.4, 69.4, 46.6, 46.0, 32.3, 27.7, 24.7, 23.8, 21.0; IR (neat) 3290, 2979, 1714, 1374, 1177, 1104, 1037, 834, 642 cm$^{-1}$; HRMS calcd for $C_{14}H_{23}BrNO_6S$ $[M(acid) + NH_4]^+$ 412.0429, found 412.0431.

**(*S*)-3-(4-Bromophenyl)piperidin-1-ium 4-methylbenzenesulfonate (29·TsOH).** To a slurry of piperidinone **25** (10.3 g, 97.5 wt %, 39.4 mmol) in THF (100 mL) was added $NaBH_4$ (4.47 g, 118 mmol) in one portion at 0−2 °C. EtOH (6.9 mL, 118 mmol) was then added over 20 min. After a further 1 h, $BF_3$·THF (13.0 mL, 118 mmol) was added over 1 h. The temperature rose to 7.5 °C during this addition (**GAS EVOLVED**). The resulting milky solution was aged at 5 °C for 1 h then at 20−25 °C for 16 h. The reaction was then cooled to 0−5 °C then slowly quenched with 8 mL MeOH (**GAS EVOLVED**). The mixture was aged for 10 min until offgassing subsided, then 37% aq HCl (9.7 mL) was added (**EXOTHERMIC** − batch temperature rose to 17 °C during the HCl addition). The mixture was then heated to 45 °C and aged for 2 h to complete decomplexation of the product-borane complex. The mixture was cooled to 15 °C, diluted with IPAc (75 mL) and water (80 mL), then adjusted to pH 8 using 28% aq $NH_4OH$ (14 mL). The resulting biphasic mixture was aged for 1 h at 20−25 °C, then the layers were separated. To the organic layer was added water (75 mL), then the pH was adjusted to 10.5 using 50 wt % aq NaOH (∼2.5 mL). The layers were separated, and the organic layer was washed with 10% aq NaCl (1 × 50 mL), filtered, and solvent-switched by distillation under vacuum at 35−40 °C (bath temperature) into IPAc to a final volume of ∼90 mL. HPLC assay gave 9.4 g (37.4 mmol, 96% yield) of piperidine **29**. The IPAc solution was heated to 40 °C, and *p*-TsOH·$H_2O$ (8.2 g, 43 mmol) was added in portions over 5 min. The resulting slurry was further heated to 50 °C, aged for 2 h, then cooled to 20−25 °C and aged for 16 h. Filtration, washing with IPAc (3 × 15 mL), and drying in vacuo at 20−25 °C under a $N_2$ sweep for 16 h afforded 14.9 g of **29·TsOH** (99.4 wt %, 96% corrected yield) as a white powder. Mp 156


dx.doi.org/10.1021/op400233z | *Org. Process Res. Dev.* 2014, 18, 215−227

°C; HPLC $t_R$ 1.2 (*p*-TsOH), 2.4 (piperidine **29**) min; $[\alpha]^{25}_D$ +5.0 (*c* 0.24, DMSO); $^1$H NMR (400 MHz, DMSO-$d_6$) $\delta$ 8.84 (br d, *J* = 10.5 Hz, 1H), 8.51 (br d, *J* = 10.5 Hz, 1H), 7.55−7.49 (m, 4H), 7.24−7.21 (m, 2H), 7.14 (dd, *J* = 8.5, 1.0 Hz, 2H), 3.28 (br t, *J* = 10.0, 10.0 Hz, 2H), 3.04−2.85 (m, 3H), 2.28 (s, 3H), 1.88−1.76 (m, 2H), 1.73−1.62 (m, 2H); $^{13}$C NMR (101 MHz, DMSO-$d_6$) $\delta$ 145.0, 141.2, 138.3, 131.6, 129.5, 128.3, 125.6, 120.2, 47.9, 43.1, 38.7, 29.2, 22.3, 20.9; IR (neat) 2944, 2816, 1609, 1488, 1222, 1159, 1117, 1006, 678 cm$^{-1}$; HRMS calcd for $C_{11}H_{15}BrN$ $[M + H]^+$ 240.0388, found 240.0381.

**(*S*)-*tert*-Butyl 3-(4-Bromophenyl)piperidine-1-carboxylate (31).** *Method A: From Tosylate Salt **29**·TsOH.* NaOH (1 N aq 72.7 mL, 72.7 mmol) was charged to a slurry of tosylate salt **29**·**TsOH** (25 g, 60.6 mmol) in MTBE (375 mL) at 20−25 °C. After 5 min $Boc_2O$ (13.4 mL, 57.6 mmol) was added over 3 min to the biphasic mixture (temperature rose from 20 to 24 °C during the addition). After aging for a further 4.5 h, the layers were separated. The organic layer was washed with water (2 × 100 mL), filtered, diluted with DMAc (100 mL), and concentrated by distillation under vacuum at 30 °C (bath temperature) to give 120 g of a clear solution (HPLC assay 21.9 g Boc-piperidinone **31**, 18.2 wt % solution) that was used directly in the C−N coupling step. For characterization, a sample of product **31** was isolated by flash column chromatography on silica gel (gradient elution from 20:1 to 10:1 *n*-hexane/MTBE), affording a colorless oil that crystallized slowly upon standing at 20−25 °C. Mp 43 °C. HPLC $t_R$ 6.39 min; $[\alpha]^{25}_D$ −62.4 (*c* 0.37, $CHCl_3$); $^1$H NMR (400 MHz, $CDCl_3$) $\delta$ 7.44 (d, *J* = 8.5 Hz, 2H), 7.11 (d, *J* = 8.5 Hz, 2H), 4.15 (t, *J* = 12.0, 12.0 Hz, 2H), 2.78−2.61 (m, 3H), 2.02−1.99 (m, 1H), 1.78−1.73 (m, 1H), 1.65−1.54 (m, 2H), 1.47 (s, 9H); $^{13}$C NMR (101 MHz, $CDCl_3$) $\delta$ 154.8, 142.5, 131.5, 128.8, 120.3, 79.6, 50.3, 44.1, 42.0, 31.7, 28.5, 25.3; IR (neat) 2939, 2857, 1685, 1418, 1362, 1136, 820, 765 cm$^{-1}$; HRMS calcd for $C_{16}H_{23}BrNO_2$ $[M + H]^+$ 340.0912, found 340.0920.

*Method B: From Mesylate **38**.* To a solution of mesylate **38** (200 mg, 0.46 mmol) in DMF (2 mL) was added powdered NaOH (31 mg, 0.78 mmol) in one portion at 22 °C. After aging for 22 h, HPLC assay indicated 146 mg of piperidine product **31** in solution (94% assay yield). The mixture was not processed further.

**3-(4-Bromophenyl)tetrahydro-2*H*-pyran-2-one (34).** A solution of acid **32** (24.2 g, 112 mmol) in THF (400 mL) was cooled to −50 °C and MeLi (72 mL of a 3 M solution in diethoxymethane, 216 mmol) was added over 20 min, maintaining the temperature between −50 and −40 °C. The slurry was then warmed to −5 °C over 1 h, and 1-bromo-3-chloropropane (12.1 mL, 123 mmol) added over 5 min at −5 to 0 °C. The batch was then aged at 0−5 °C for 1.5 h before being quenched by the addition of 1 M aq NaOH (160 mL) in one portion (temperature rose from 5 to 14 °C). The mixture was concentrated by distillation under vacuum at 35 °C (bath temperature) to remove most of the THF, and the residue was partitioned between 1:1 v/v *n*-heptane/MTBE (100 mL) and water (50 mL). The layers were separated, and the aqueous layer was adjusted to pH 1 using 37% aq HCl. The aqueous layer was extracted with EtOAc (2 × 150 mL), and the combined organic layers were washed with water (1 × 100 mL), dried over $MgSO_4$, filtered and concentrated to afford 35.33 g of crude acid **33** (89.6 HPLC area% purity) as a colorless oil. This oil was dissolved in EtOAc (235 mL) at 25 °C and DBU (16.9 mL, 112 mmol) was added in two portions over 5 min (temperature rose from 25 to 36 °C over 5 min). The batch was then heated to 63−65 °C and aged for 3 h, before being allowed to cool to 22 °C overnight. The slurry was then filtered, washing the cake with EtOAc (1 × 100 mL), and the combined filtrates were concentrated to afford an orange solid which was purified by flash chromatography on silica gel (gradient elution from 3:1 to 1:1 hexanes/EtOAc). Product-containing fractions were concentrated and the residue slurried in 3:1 v/v hexanes/EtOAc (60 mL) at 22 °C for 2 h. Filtration and drying in vacuo at 22 °C under a $N_2$ sweep for 5 h afforded 22.95 g of **34** (80% overall yield) as a white powder. Mp 78−79 °C; HPLC $t_R$ 4.0 min; $^1$H NMR (500 MHz, $CDCl_3$) $\delta$ 7.50−7.47 (m, 2H), 7.14−7.11 (m, 2H), 4.50−4.42 (m, 2H), 3.77−3.72 (m, 1H), 2.32−2.25 (m, 1H), 2.08−1.98 (m, 3H); $^{13}$C NMR (126 MHz, $CDCl_3$) $\delta$ 171.9, 137.8, 131.8, 130.0, 121.3, 69.1, 46.5, 28.0, 22.0; IR (neat) 2938, 1723, 1487, 1152, 1071, 1010, 809 cm$^{-1}$; HRMS calcd for $C_{11}H_{12}BrO_2$ $[M + H]^+$ 255.0021, found 255.0019.

**3-(4-Bromophenyl)tetrahydro-2*H*-pyran-2-ol (35).** A solution of lactone **34** (20.3 g, 80 mmol) in 1:1 v/v PhMe/THF (140 mL) was cooled to −18 °C, and a solution of DIBAL (55.7 mL of a 1 M solution in PhMe, 84 mmol) was added over 70 min, maintaining the temperature between −18 and −8 °C. The batch was aged at −15 °C for a further 50 min before being quenched by the addition of 2 M aq HCl (10 mL) over 5 min (temperature rose from −13 to −5 °C). Additional 2 M aq HCl (120 mL) was then added over 1 min (temperature rose from −5 to 15 °C). The mixture was aged at 22 °C for 1 h, then the layers were separated. The organic layer was washed with water (1 × 80 mL), filtered and concentrated to dryness. The residue was dissolved in toluene (21 mL) at 22 °C, and *n*-heptane (21 mL) was added. Seed crystals of lactol product **35** (50 mg) were added, and the slurry aged overnight. *n*-Heptane (60 mL) was added over 2 h, and the slurry was aged at 22 °C for 5 h before being cooled to 5 °C and aged for a further 1 h. Filtration, washing with *n*-heptane (2 × 30 mL), and drying in vacuo at 22 °C under a $N_2$ sweep for 5 h afforded 18.68 g of **35** (97 wt % purity, 89% corrected yield) as a white powder and as a ∼2:1 mixture of anomers. Mp 71−72 °C; HPLC $t_R$ 3.82 min; $^1$H NMR (400 MHz, $CDCl_3$) $\delta$ 7.46−7.41 (m, 2H (major anomer) and 2H (minor anomer)), 7.20 (d, *J* = 8.5 Hz, 2H (minor)), 7.15−7.12 (m, 2H (major)), 5.18 (d, *J* = 3.0 Hz, 1H (minor)), 4.74 (d, *J* = 8.0 Hz, 1H (major)), 4.09−4.02 (m, 1H (major) and 1H (minor)), 3.64−3.58 (m, 1H (major) and 1H (minor)), 3.31 (br s, 1H (minor)), 2.94 (dt, *J* = 12.5, 3.0 Hz, 1H (minor)), 2.61−2.55 (m, 1H (major)), 2.27−2.16 (m, 1H (minor)), 2.02−1.96 (m, 1H (major)), 1.84−1.65 (m, 3H (major) and 3H (minor)); $^{13}$C NMR (101 MHz, $CDCl_3$) $\delta$ 140.6 (major), 140.6 (minor), 131.4 (major), 131.2 (minor), 130.0 (minor), 129.6 (major), 125.5 (minor), 120.4 (major), 98.7 (major), 93.8 (minor), 66.0 (major), 59.3 (minor), 48.5 (major), 46.1 (minor), 30.0 (major), 25.5 (minor), 25.0 (major), 22.9 (minor); IR (neat) 3257, 2929, 2856, 1488, 1051, 1010, 980, 808 cm$^{-1}$; HRMS calcd for $C_{11}H_{13}BrNaO_2$ $[M + Na]^+$ 278.9997, found 279.0007.

**(*S*)-*tert*-Butyl (2-(4-Bromophenyl)-5-hydroxypentyl)-carbamate (37).** Pyridoxal-5-phosphate (0.4 g, 1.6 mmol) was dissolved in 0.2 M aq borate buffer (320 mL) containing 1 M aq *i*-$PrNH_2$ was added at 22 °C. To the resulting solution (pH 8.5) was charged ATA-301 enzyme (4 g) with gentle agitation. Once the enzyme had fully wetted, DMSO (40 mL) was added, and the mixture was heated to 45 °C. A solution of lactol **35** (10 g, 38.9 mmol) in DMSO (40 mL) was added over 5 min. The mixture was aged at 45 °C for 69 h, during which


dx.doi.org/10.1021/op400233z | *Org. Process Res. Dev.* 2014, 18, 215−227

time the pH was maintained at 8.5 by addition of 4 M aq *i*-$PrNH_2$, before being cooled to 25 °C. Solka-Floc (5 g) was added, and the pH of the mixture adjusted to 2.5 using 6 N aq HCl. The mixture was aged for 1 h then filtered. The aqueous filtrate (~500 mL, containing crude amine **36** at 97.4 HPLC area% purity) was washed with EtOAc (1 × 400 mL), and then adjusted to pH 10 using 10 M aq NaOH. $Boc_2O$ (13.6 g, 62.2 mmol) was added in one portion at 22 °C, and the mixture aged for 30 min before being extracted with MTBE (1 × 600 mL). The organic layer was washed with water (1 × 200 mL), sat aq NaCl (1 × 200 mL), dried over $MgSO_4$, filtered and concentrated to afford crude alcohol **37** (85 wt % purity, 95 HPLC area% purity) as a yellow oil that was used directly in the subsequent mesylation step. Data for crude alcohol **37**: HPLC $t_R$ 4.51 min; $^1$H NMR (500 MHz, $CDCl_3$) $\delta$ 7.46−7.44 (m, 2H), 7.06 (d, $J$ = 8.5 Hz, 2H), 4.40 (br s, 1H), 3.59−3.58 (br m, 2H), 3.48−3.46 (br m, 1H), 3.15 (ddd, $J$ = 14.0, 8.5, 5.0 Hz, 1H), 2.76 (br s, 1H), 1.81−1.74 (m, 1H), 1.63−1.56 (m, 1H), 1.53−1.42 (m, 3H), 1.40 (s, 9H); $^{13}$C NMR (126 MHz, $CDCl_3$) $\delta$ 155.9, 141.6, 131.8, 129.6, 120.5, 79.4, 62.6, 46.1, 45.5, 30.3, 29.5, 28.3.

**(*S*)-4-(4-Bromophenyl)-5-((*tert*-butoxycarbonyl)-amino)pentyl Methanesulfonate (38).** The crude alcohol **37**, prepared as described above, was dissolved in $CH_2Cl_2$ (120 mL) and cooled to 5 °C. $Et_3N$ (10.8 mL, 78 mmol) was added in one portion, followed by the addition of MsCl (3.6 mL, 46.7 mmol) over 3 min. The slurry was aged at 5 °C for 30 min before being poured into 0.8 M aq HCl (70 mL) at 22 °C. The layers were separated, and the organic layer was washed with 1:1 sat aq NaCl/sat aq $NaHCO_3$ (1 × 70 mL), dried over $MgSO_4$, filtered and concentrated. The residue was dissolved in 3:2 hexanes/EtOAc (25 mL) at 22 °C, which was followed by rapid crystallization of the product. Additional EtOAc (10 mL) was added, and the slurry aged overnight. Hexanes (25 mL) was added over 75 min, and the slurry aged for a further 4 h. Filtration, washing with 9:1 hexanes/EtOAc (1 × 20 mL) followed by hexanes (1 × 20 mL), and drying in vacuo at 22 °C under a $N_2$ sweep overnight afforded 8.2 g of **38** (99.4 wt % purity, 48% overall yield from lactol **35**) as a cream powder. Mp 98 °C; HPLC $t_R$ 5.07 min; $[\alpha]^{25}_D$ − 36.6 ($c$ 1.07, $CHCl_3$); $^1$H NMR (400 MHz, $CDCl_3$) $\delta$ 7.47−7.44 (m, 2H), 7.06−7.03 (m, 2H), 4.44 (br s, 1H), 4.15 (t, $J$ = 6.0 Hz, 2H), 3.44 (br s, 1H), 3.16−3.11 (m, 1H), 2.97 (s, 3H), 2.76 (br s, 1H), 1.83−1.76 (m, 1H), 1.68−1.56 (m, 3H), 1.40 (s, 9H); $^{13}$C NMR (101 MHz, $CDCl_3$) $\delta$ 155.8, 140.9, 131.9, 129.5, 120.7, 79.4, 69.5, 46.0, 45.2, 37.3, 29.0, 28.3, 26.9; IR (neat) 3387, 2983, 2931, 1677, 1517, 1347, 1168, 918, 775 cm$^{-1}$; HRMS calcd for $C_{17}H_{27}BrNO_5S$ $[M + H]^+$ 436.0793, found 436.0802.

***N*-(*tert*-Butyl)-1*H*-indazole-7-carboxamide (46).** CDI (59.1 g, 97 wt %, 354 mmol) was added to a solution of indazole **41** (50.3 g, 95 wt %, 295 mmol) in DMF (150 mL) at 20−25 °C (**GAS EVOLVED**). After 30 min, moderate vacuum (50−100 mmHg) was briefly applied to the reaction mixture to ensure complete removal of the $CO_2$ byproduct. After a further 25 min, *t*-$BuNH_2$ (62.5 mL, 589 mmol) was added over 3 min (**EXOTHERMIC**). With no external cooling, the batch temperature rose from 21 to 38 °C over 40 min. The mixture was then aged at 40 °C for a further 2.5 h. After cooling to 20 °C, water (100 mL) was added, maintaining the temperature below 25 °C. The solution was then seeded with crystalline product **46** (150 mg), and the slurry was aged at 20−25 °C for 30 min. Water (500 mL) was then added over 80 min, and the slurry aged overnight. Filtration, washing with 9:1 v/v water/DMF (1 × 250 mL) followed by water (2 × 250 mL), and drying in vacuo at 20−25 °C under a $N_2$ sweep afforded 55.3 g of **46** (86% yield) as a beige powder. Mp 158.5−159 °C; HPLC $t_R$ 3.47 min; $^1$H NMR (400 MHz, $CDCl_3$) $\delta$ 13.07 (br s, 1H), 8.17 (s, 1H), 8.03 (br s, 1H), 7.92 (d, $J$ = 7.5 Hz, 1H), 7.91 (d, $J$ = 7.5 Hz, 1H), 7.15 (t, $J$ = 7.5 Hz, 1H), 1.45 (s, 9H); $^{13}$C NMR (101 MHz, DMSO-$d_6$) $\delta$ 165.7, 138.5, 132.8, 125.5, 124.1, 119.7, 118.8, 51.0, 28.7; IR (neat) 3442, 3374, 2960, 1665, 1649, 1513, 1298, 941, 843, 748, 713 cm$^{-1}$; HRMS calcd for $C_{12}H_{16}N_3O$ $[M + H]^+$ 218.1293, found 218.1292.

**(*S*)-*tert*-Butyl 3-(4-(7-(*tert*-Butylcarbamoyl)-2*H*-indazol-2-yl)phenyl)piperidine-1-carboxylate (56).** To 113 g of crude Boc-piperidinone **31** solution (18.2 wt % in DMAc, 20.6 g **31**, 60.6 mmol) was charged indazole **46** (13.8 g, 63.6 mmol) and $K_2CO_3$ (25.6 g, 182 mmol) at 20−25 °C. Additional DMAc (10 mL) was used to wash residual solids down into the flask. The mixture was degassed by subsurface sparging with $N_2$ for 1 h. CuBr (0.444 g, 3.03 mmol) and 8-hydroxyquinoline **52** (0.889 g, 6.06 mmol) were added, and $N_2$ sparging continued for 30 min. The mixture was then heated to 110 °C and aged for 24 h. After cooling to 40 °C, Celite (14.5 g) was added, and the mixture aged for 1 h before being filtered, washing the cake with DMAc (1 × 100 mL). The combined filtrates (HPLC assay 28.6 g **56**, 99% yield) were adjusted to 35 °C, then DMAc (50 mL) and 10% aq citric acid (26 mL) were added, followed by seed crystals (286 mg) of product **56**. After 1 h additional 10% aq citric acid (60 mL) was added over 100 min. The resulting slurry was aged for 2 h at 35 °C then at 20−25 °C overnight. Filtration, washing with 2:1 v/v DMAc/water (1 × 150 mL) followed by water (1 × 300 mL), and drying in vacuo at 20−25 °C under a $N_2$ sweep afforded 27.24 g of **56** (98.3 wt %, 94% corrected yield) as a light-yellow powder. Mp 192 °C; HPLC $t_R$ 6.49 min; $[\alpha]^{25}_D$ −62.8 ($c$ 0.25, DMSO); $^1$H NMR (400 MHz, MeOH-$d_4$) $\delta$ 9.57 (s, 1H), 8.94 (s, 1H), 8.09 (dd, $J$ = 7.0, 1.0 Hz, 1H), 7.96 (d, $J$ = 8.5 Hz, 2H), 7.95 (dd, $J$ = 8.5, 1.0 Hz, 1H), 7.50 (d, $J$ = 8.5 Hz, 2H), 7.23 (dd, $J$ = 8.5, 7.0 Hz, 1H), 4.17−4.09 (br m, 2H), 2.91−2.86 (br m, 2H), 2.79−2.73 (m, 1H), 2.05 (d, $J$ = 12.0 Hz, 1H), 1.82−1.72 (m, 2H), 1.64−1.60 (m, 1H), 1.58 (s, 9H), 1.48 (s, 9H); $^{13}$C NMR (101 MHz, MeOH-$d_4$) $\delta$ 166.6, 156.7, 147.9, 145.7, 139.9, 130.7, 129.8, 126.5, 125.3, 124.0, 123.3, 121.8, 81.3, 52.7, 43.7, 32.9, 29.5, 28.9, 26.6; IR (neat) 3300, 3102, 2933, 2849, 1684, 1649, 1572, 1363, 1172, 833, 749 cm$^{-1}$; HRMS calcd for $C_{28}H_{37}N_4O_3$ $[M + H]^+$ 477.2866, found 477.2878.

**Niraparib *p*-Toluenesulfonate Monohydrate (9).**[3] All operations in this step were performed in a dedicated potent compound-handling facility.

To a slurry of amide **56** (20.0 g, 98.3 wt %, 41.2 mmol) in *o*-xylene (40 mL) was charged MSA (60 mL, 924 mmol) at 22 °C (**GAS EVOLVED**; **EXOTHERMIC**—with no external cooling the batch temperature rose from 22 to 36 °C over 5 min). After 5 min the biphasic mixture was warmed to 40 °C, aged for 2.5 h, then cooled to below 20 °C. Water (140 mL) was added over 23 min, maintaining the temperature below 25 °C. The layers were then separated, and the aqueous layer was washed with PhMe (1 × 20 mL) and filtered. A solution of *p*-TsOH·$H_2O$ (11.8 g, 61.9 mmol) in water (23.5 mL) was prepared, and 6 mL added over 20 min to the aqueous filtrate at 20 °C. Seed crystals of product salt **9** (400 mg) were introduced, and the resulting slurry aged for 30 min. The remainder of the aq *p*-TsOH solution was then added over 75 min, and the mixture aged overnight. Filtration, washing with water (3 × 100 mL), and drying in vacuo at 20−25 °C under a $N_2$ sweep overnight


dx.doi.org/10.1021/op400233z | *Org. Process Res. Dev.* 2014, 18, 215−227

afforded 20.6 g of **9** (99.8 HPLC area % purity, 97.3 wt %, 95% corrected yield) as white powder.

## ■ ASSOCIATED CONTENT

### Supporting Information

Procedure for the preparation of solid bisulfite adduct **28**, chiral SFC analysis of piperidinone **25**, chiral HPLC analysis of aminoalcohol **36**, and copies of $^{1}H$ and $^{13}C$ NMR spectra for all new compounds. This material is available free of charge via the Internet at http://pubs.acs.org.

## ■ AUTHOR INFORMATION


### Corresponding Authors

*E-mail: cheol_chung@merck.com.
*E-mail: paul_bulger@merck.com


### Notes

The authors declare no competing financial interest.

## ■ ACKNOWLEDGMENTS

We thank Dr. Tom J. Novak for assistance with HRMS analysis, Zainab Pirzada and Tanja Brkovic for analytical support, and Cheng-yi Chen, Pintipa Grongsaard, Phil Jones and Debra J. Wallace for helpful discussions.

## ■ REFERENCES


(1) Jagtap, P.; Szabó, C. *Nat. Rev. Drug Discovery* **2005**, *4*, 421−440.

(2) (a) Kummar, S.; Chen, A.; Parchment, R. E.; Kinders, R. J.; Ji, J.; Tomaszewski, J. E.; Doroshow, J. H. *BMC Medicine* **2012**, *10*, 25−29. (b) Park, S. R.; Chen, A. *Hematol. Oncol. Clin. N. Am.* **2012**, *26*, 649−670. (c) Smith, K. L.; Isaacs, C. *Curr. Breast Cancer Rep.* **2011**, *3*, 165−171.

(3) Wallace, D. J.; Baxter, C. A.; Brands, K. J. M.; Bremeyer, N.; Brewer, S. E.; Desmond, R.; Emerson, K. M.; Foley, J.; Fernandez, P.; Hu, W.; Keen, S. P.; Mullens, P.; Muzzio, D.; Sanjoz, P.; Tan, L.; Wilson, R. D.; Zhou, G.; Zhou, G. *Org. Process Res. Dev.* **2011**, *15*, 831−840.

(4) Jones, P.; Altamura, S.; Boueres, J.; Ferrigno, F.; Fonsi, M.; Giomini, C.; Lamartina, S.; Monteagudo, E.; Ontoria, J. M.; Orsale, M. V.; Palumbi, M. C.; Pesci, S.; Roscilli, G.; Scarpelli, R.; Schultz-Fademrecht, C.; Toniatti, C.; Rowley, M. *J. Med. Chem.* **2009**, *52*, 7170−7185.

(5) Antilla, J. C.; Baskin, J. M.; Barder, T. E.; Buchwald, S. L. *J. Org. Chem.* **2004**, *69*, 5578−5587.

(6) (a) Joubert, N.; Baslé, E.; Vaultier, M.; Pucheault, M. *Tetrahedron Lett.* **2010**, *51*, 2994−2997. (b) Hari, Y.; Shoji, Y.; Aoyama, T. *Tetrahedron Lett.* **2005**, *46*, 3771−3774. (c) Lam, P. Y. S.; Vincent, G.; Clark, C. G.; Deudon, S.; Jadhav, P. K. *Tetrahedron Lett.* **2001**, *42*, 3415−3418. (d) Lam, P. Y. S.; Clark, C. G.; Saubern, S.; Adams, J.; Winters, M. P.; Chan, D. M. T.; Combs, A. *Tetrahedron Lett.* **1998**, *39*, 2941−2944.

(7) Selected examples: (a) Chiral auxiliary-mediated DKR: Amat, M.; Cantó, M.; Llor, N.; Escolano, C.; Molins, E.; Espinosa, E.; Bosch, J. *J. Org. Chem.* **2002**, *67*, 5343−5351. (b) Alkene hydrogenation: Verendel, J. J.; Zhou, T.; Li, J.-Q.; Paptchikhine, A.; Lebedev, O.; Andersson, P. G. *J. Am. Chem. Soc.* **2010**, *132*, 8880−8881. (c) Asymmetric alkylation: Michon, C.; Béthegnies, A.; Capet, F.; Roussel, P.; de Filippis, A.; Gomez-Pardo, D.; Cossy, J.; Agbossou-Niedercorn, F. *Eur. J. Org. Chem.* **2013**, 4979−4985.

(8) For reviews and selected applications, see: (a) Savile, C. K.; Janey, J. M.; Mundorff, E. C.; Moore, J. C.; Tam, S.; Jarvis, W. R.; Colbeck, J. C.; Krebber, A.; Fleitz, F. J.; Brands, J.; Devine, P. N.; Huisman, G. W.; Hughes, G. J. *Science* **2010**, *329*, 305−309. (b) Mutti, F. G.; Kroutil, W. *Adv. Synth. Catal.* **2012**, *354*, 3409−3413. (c) Berglund, P.; Humble, M. S.; Branneby, C. *Comprehensive Chirality*; Carreria, E. M., Yamamoto, H., Eds.; Elsevier; Amsterdam, 2012; Vol. 7, pp 390−401.

(9) (a) Ohkuma, T.; Li, J.; Noyori, R. *Synlett* **2004**, 1383−1386. (b) Chung, J. Y. L.; Mancheno, D.; Dormer, P. G.; Variankaval, N.; Ball, R. G.; Tsou, N. N. *Org. Lett.* **2008**, *10*, 3037−3040. (c) Xu, F.; Chung, J. Y. L.; Moore, J. C.; Liu, Z.; Yoshikawa, N.; Hoerrner, R. S.; Lee, J.; Royzen, M.; Cleator, E.; Gibson, A. G.; Dunn, R.; Maloney, K. M.; Alam, M.; Goodyear, A.; Lynch, J.; Yasuda, N.; Devine, P. N. *Org. Lett.* **2013**, *15*, 1342−1345.

(10) Koszelewski, D.; Clay, D.; Faber, K.; Kroutil, W. *J. Mol. Catal. B: Enzym.* **2009**, *60*, 191−194.

(11) The asymmetric reductive amination of aldehydes via DKR using small-molecule organocatalysis had previously been reported by List and co-workers: Hoffmann, S.; Nicoletti, M.; List, B. *J. Am. Chem. Soc.* **2006**, *128*, 13074−13075.

(12) Seed, A. J.; Sonpatki, V.; Herbert, M. R. *Org. Synth.* **2002**, *79*, 204−206.

(13) (a) Rubin, A. E.; Tummala, S.; Both, D. A.; Wang, C.; Delaney, E. J. *Chem. Rev.* **2006**, *106*, 2794−2810. (b) Shultz, C. S.; Krska, S. W. *Acc. Chem. Res.* **2007**, *40*, 1320−1326. (c) Belyk, K. M.; Xiang, B.; Bulger, P. G.; Leonard, W. R., Jr.; Balsells, J.; Yin, J.; Chen, C. *Org. Process Res. Dev.* **2010**, *14*, 692−700.

(14) The use of $ZnBr_2$ in PhMe to promote epoxide rearrangement has been reported previously. For an example, see: Ramachandran, P. V.; Krzeminski, M. P. *Tetrahedron Lett.* **1999**, *40*, 7879−7881.

(15) The *y*-axis values refer to the HPLC area % ratios of desired product to an internal reference standard, and are a qualitative measure of relative reaction performance.

(16) Available from Codexis, Inc., 200 Penobscot Drive, Redwood City, CA 94063, United States.

(17) Using an alternative procedure (see the Supporting Information), solid bisulfite adduct **28** could be isolated by crystallization; however, the more streamlined through-process was preferred.

(18) (a) Guercio, G.; Manzo, A. M.; Goodyear, M.; Bacchi, S.; Curti, S.; Provera, S. *Org. Process Res. Dev.* **2009**, *13*, 489−493. (b) Atkins, W. J., Jr.; Burkhardt, E. R.; Matos, K. *Org. Process Res. Dev.* **2006**, *10*, 1292−1295.

(19) For a discussion of potential hazards associated with the use of $BH_3$·THF on scale, see: am Ende, D. J.; Vogt, P. F. *Org. Process Res. Dev.* **2003**, *7*, 1029−1033.

(20) For experimental details, see the Supporting Information. Note that different vessel configurations and headspace nitrogen sweep conditions may give different concentrations of diborane exiting the reactor.

(21) Rosen, J. D.; Nelson, T. D.; Huffman, M. A.; McNamara, J. M. *Tetrahedron Lett.* **2003**, *44*, 365−368.

(22) (a) Pu, Y.-M.; Ku, Y.-Y.; Grieme, T.; Henry, R.; Bhatia, A. V. *Tetrahedron Lett.* **2006**, *47*, 149−153. (b) Pu, Y.-M.; Ku, Y.-Y.; Grieme, T.; Black, L. A.; Bhatia, A. V.; Cowart, M. *Org. Process Res. Dev.* **2007**, *11*, 1004−1009.

(23) Burgos, C. H.; Barder, T. E.; Huang, X.; Buchwald, S. L. *Angew. Chem., Int. Ed.* **2006**, *45*, 4321−4326.

(24) See: Wang, Z.; Richter, S. M.; Gates, B. D.; Grieme, T. A. *Org. Process Res. Dev.* **2012**, *16*, 1994−2000 and references therein.